CERN-TH/95-246

Initial State QED Corrections to W-pair Production at LEP2/NLC — Monte Carlo Versus Semianalytical Approach†

M. Skrzypek⋆
Institute of Nuclear Physics, Kraków, ul. Kawiory 26a, Poland
S. Jadach⋆
Institute of Nuclear Physics, Kraków, ul. Kawiory 26a, Poland
CERN, Theory Division, Geneva 23, Switzerland,
M. Martinez
IFAE, Bellaterra (Barcelona), Spain
W. Płaczek‡⋆
Department of Physics and Astronomy,
The University of Tennessee, Knoxville, TN 37996-1200
and
Z. Wąs⋆
CERN, Theory Division, Geneva 23, Switzerland,
Institute of Nuclear Physics, Kraków, ul. Kawiory 26a, Poland

Abstract

We present a comparison of the Monte Carlo code KORALW with the SemiANalytical code KORWAN for W-pair production. We focus on the technical precision, total cross section and some differential distributions. We find the technical precision of KORALW in the LEP2 energy range to be of order 10^{-4} or better. We show that within the 0.1% precision level the $\mathcal{O}(\alpha^2)$ photonic corrections are not necessary in the YFS framework, at least for the total cross section.

A detailed description of the semianalytical formalism implemented in the KORWAN routine is also given.

To be submitted to Physics Letters

---

† Work supported in part by Polish Government grant KBN 2P30225206 and European Commission contract ERBCIPDCT940016.

‡ On leave of absence from *Institute of Computer Science, Jagellonian University, Kraków, ul. Reymonta 4, Poland*

⋆ `www` home page at `http://hpjmiady.ifj.edu.pl/`

CERN-TH/95-246
September 1995

1 Introduction

With the forthcoming increase of the LEP energy, new processes like W-pair production and decay will offer opportunities for an experimental investigation of fundamental quantities such as W mass or triple boson coupling. During the preparation for the first phase of LEP operation [1], at centre-of-mass energies comparable with the Z mass, it was advocated that different classes of radiative corrections may turn out to be essential in the interpretation of experimental results. Indeed, in some cases such as the τ polarization measurement [2], Monte Carlo modelling of the observables is important. In the case of the luminosity measurement at LEP1 [3] QED corrections constitute, even today, the systematic uncertainty surpassing the experimental error and limiting the physical significance of the measurement of the number of neutrino species. The main difficulty is the complicated interrelation of experimental cuts and strongly peaked multiphoton phase space, which has to be handled with the help of a high-precision Monte Carlo simulation.

It is thus of high practical importance to ensure that a similar situation will not repeat at LEP2 and, if necessary, to take appropriate steps in advance. For this purpose a whole family of Monte Carlo programs and semi-analytical calculations are being developed (see e.g. [4, 5, 6, 7]) and are being studied by the LEP2 workshop [8]. In the future W-pair production and decay measurements we expect to reach the 1% experimental precision level. For theoretical effects to be negligible, theoretical predictions of the Standard Model have to be given with precision, which is at least 0.5% and preferably 0.3%. Due to complicated cuts which are usually applied in experimental analyses, a Monte Carlo representation of the theoretical results is necessary.

The purpose of the present paper is twofold. First, a technical one is to check if the Monte Carlo program KORALW [9] for W-pair production and decay in the LEP2 energy range is reproducing some distributions calculated using different methods, that is semi-analytical calculation. The second is to study the size of some well-defined class of initial-state QED corrections for the total cross section of W-pairs as a function of the centre-of-mass energy.

Good agreement, on a level significantly better than 0.1% (in fact better than 0.01%!), defines a solid starting point for inclusion of smaller corrections into the Monte Carlo program, as well as for the discussion of theoretical uncertainties due to further missing terms, for observables of direct experimental and phenomenological interest.

2 Semi-analytical Calculation

The core of the tests of the Monte Carlo (MC) code KORALW is the comparison with the dedicated semi-analytical (SAN) calculation. These two approaches are completely different both in their principles (helicity amplitudes with YFS resummation of soft photons versus standard Feynman diagram calculation plus Structure

Functions) and in their numerical implementation (MC integration versus Gaussian integration). Therefore they form an excellent tool for mutual tests. This approach has however certain limitations. Namely, the SAN calculation cannot handle complicated cuts required by the real experiment. In fact, in our SAN formalism no angular cuts of any kind can be applied. The only variables available for cuts are the total energy carried away by photons: $v = 1 - s'/s$ and two invariant masses of the virtual W bosons: s_1, s_2. This limits our comparisons with the quantities like total cross section or differential cross sections with respect to the v and s_i variables.

The extensive presentation of the MC algorithm and program was done in ref. [9]. Also a brief description of the SAN calculation can be found therein. In the following we will give a more detailed description of the SAN calculation.

Let us start with a presentation of the master analytical formula and discuss in detail its components:

$$\sigma^{SAN}(v_{min}, v_{max}) = N_S \int\limits_{1-v_{max}}^{1-v_{min}} dx F(x,s) \int\limits_0^{xs} ds_1 \int\limits_0^{(\sqrt{xs}-\sqrt{s_1})^2} ds_2 \, \rho(s_1)\, \rho(s_2)\, \sigma_0^S(xs, s_1, s_2). \tag{1}$$

The hard cross section $\sigma_0^S(xs, s_1, s_2)$ is taken from ref. [10]. The only modification that had to be done to the original formula of eq. (4) in ref. [10] was to modify the appropriate Z propagators. For the sake of completeness we present the complete modified formula for σ_0^S in the Appendix. The functions $\rho(s_i)$ in eq. (1) are also modified with respect to ref. [10]:

$$\rho(s_i) = \frac{1}{\pi}\frac{1}{12}\frac{\alpha_W}{\sin^2\theta_W}\frac{s_i}{(s_i - M_W^2)^2 + s_i^2\Gamma_W^2/M_W^2}. \tag{2}$$

To adjust the overall normalization of the cross section to the convention of the KORALW MC program, the corrective factor N_S is introduced in eq. (1) for the specific (a,b) decay channel

$$N_S = \left(\frac{BR_a}{BR_{(e\nu)}}\right)\left(\frac{BR_b}{BR_{(e\nu)}}\right). \tag{3}$$

The $BR_{(e\nu)}$ denotes the branching ratio of the single W into the $e\nu$ channel, and BR_a is the branching ratio into an arbitrary a channel; α_W denotes the QED coupling constant at the WW threshold, and $\sin\theta_W$ is the sine of the Weinberg angle.

Finally, we need to discuss the Initial State Radiation (ISR) kernel $F(x,s)$. Since in the radiative sector we are working within the Leading Logarithmic (LL) approximation the $F(x,s)$ kernel is defined in the standard way as a convolution of two Structure Functions $D(x_i, s)$:

$$F(x,s) = \int\limits_0^1 dx_1 dx_2 \delta(x - x_1 x_2) D(x_1, s) D(x_2, s). \tag{4}$$

There are a variety of representations of the exponentiated Structure Functions available in the literature. They range from the standard, second-order ones exponentiated according to the Kuraev-Fadin (KF) [11] classical prescription, to the third-order, faster convergent ones exponentiated according to the Jadach-Ward (JW) prescription of refs. [12, 13, 14]. Any of these functions can be used to construct the kernel $F(x,s)$ of eq. (4). Among others both of the above mentioned functions are implemented in the actual FORTRAN routine KORWAN. One has to remember, however, that the main objective of our analytical calculation is to cross-check the MC results. In order to achieve this, the kernel $F(x,s)$ has to be slightly modified to account for some non-leading terms present in the YFS scheme and by definition absent or ambiguous in LL Structure Functions. Let us show these modifications on the example of the second-order kernel $F_{JW}^{(2)}(x,s)$ exponentiated according to the Jadach-Ward prescription of ref. [12]:

$$
\begin{aligned}
F_{JW}^{(2)}(1-v,s) &= N_{NLL}N_{YFS}\frac{e^{-C_{Euler}\beta_i}}{\Gamma(1+\beta_i)}\beta_i v^{\beta_i-1}\Delta_{JW}^{(2)}, && (5)\\
\beta_i &= 2\frac{\alpha}{\pi}\Big(\log\frac{s}{m_e^2}-1\Big), && (6)\\
N_{YFS} &= \exp\Big(\frac{1}{4}\beta_i\Big), && (7)\\
N_{NLL} &= \exp\Big[\frac{\alpha}{\pi}\Big(-\frac{1}{2}+\frac{\pi^2}{3}\Big)\Big], && (8)\\
\Delta_{JW}^{(2)} &= \langle\bar{\beta}_0^{(2)}\rangle+\langle\bar{\beta}_1^{(2)}\rangle+\langle\bar{\beta}_2^{(2)}\rangle, && (9)\\
\langle\bar{\beta}_0^{(2)}\rangle &= 1+\frac{\beta_i}{2}+\frac{\beta_i^2}{8}-\frac{\beta_i}{4}\log(1-v), && (10)\\
\langle\bar{\beta}_1^{(2)}\rangle &= v\Big(\frac{v}{2}-1\Big)-\frac{\beta_i}{2}\Big(\frac{1}{4}(2-6v+3v^2)\log(1-v)+v+\frac{1}{2}v^2\Big), && (11)\\
\langle\bar{\beta}_2^{(2)}\rangle &= \frac{\beta_i}{4}v^2. && (12)
\end{aligned}
$$

First, the explicitly non-leading form factor N_{NLL} has to be added. Next, to reproduce the proper soft limit behaviour of F, the effective LL parameter $\beta = 2\frac{\alpha}{\pi}\log\frac{s}{m_e^2}$ is to be replaced by the β_i parameter. Let us stress that the above modifications, *ad hoc* in the LL Structure Functions approach, can be understood in the YFS formulation as a result of the actual phase-space integration. This integration can be carried out even further – one can identify separate pieces $\langle\bar{\beta}_k\rangle$ of the Δ_{JW} as originating from different $\bar{\beta}_k$ terms of the YFS expansion [15], see ref. [9] for details on the definition of $\bar{\beta}$ terms. This separation turns out to be very helpful for the in-depth tests of the Monte Carlo algorithm and we show it explicitly in eq. (9). Finally, the N_{YFS} form factor differs from the well-known Gribov-Lipatov exponent $N_{GL} = \exp(\frac{3}{4}\beta_i)$. The not exponentiated $\exp(\frac{1}{2}\beta_i)$ is compensated order by order in the perturbative Δ_{JW} function.

We present here also the third-order result for the Δ_{JW} function [12, 13], modified

to account for the specific form of the N_{YFS} form factor

$$\begin{aligned}\Delta^{(3)}_{JW} &= 1+\frac{\beta_i}{2}+\frac{\beta_i^2}{8}+\frac{\beta_i^3}{48}+\Big(1+\frac{\beta_i}{2}+\frac{\beta_i^2}{8}\Big)v\Big(\frac{v}{2}-1\Big)\\ &- \Big(1+\frac{\beta_i}{2}\Big)\frac{\beta_i}{4}\Big[\frac{1}{2}\Big(1+3(1-v)^2\Big)\log(1-v)+v^2\Big]\\ &+ \frac{\beta_i^2}{8}\Big[\frac{1}{2}(3v-2)v\log(1-v)+\frac{1}{12}(8-14v+7v^2)\log^2(1-v)\\ &\qquad +v^2+(2-v)v\mathrm{Li}_2(v)\Big]. \end{aligned} \tag{13}$$

The numerical algorithm used by us to evaluate eq. (1) is the following. The inner integration variables s_1 and s_2 are changed to u_1 and u_2 according to

$$s_i = M_W\Gamma_W\tan\Big(M_W\Gamma_W u_i\Big)+M_W^2 \tag{14}$$

and integrated out by a Gaussian technique.

From the outermost integration over $v=1-x$ we subtract the singular part and integrate it by hand

$$\begin{aligned}\sigma^{sing}(v_{min},v_{max}) &= N_S\sigma^B(v_{min})N_{NLL}N_{YFS}\frac{e^{-C_{Euler}\beta_i}}{\Gamma(1+\beta_i)}\delta_s\int\limits_{v_{min}}^{v_{max}}dv\beta_i v^{\beta_i-1}\\ &= N_S\sigma^B(v_{min})N_{NLL}N_{YFS}\frac{e^{-C_{Euler}\beta_i}}{\Gamma(1+\beta_i)}\delta_s(v_{max}^{\beta_i}-v_{min}^{\beta_i}), \qquad (15)\\ \delta_s &= 1+\frac{\beta_i}{2}+\frac{\beta_i^2}{8}, \qquad (16)\end{aligned}$$

where

$$\sigma^B(v_{min}) = \int\limits_0^{(1-v_{min})s}ds_1\int\limits_0^{(\sqrt{(1-v_{min})s}-\sqrt{s_1})^2}ds_2\,\rho(s_1)\,\rho(s_2)\,\sigma_0^S((1-v_{min})s,s_1,s_2); \tag{17}$$

$\sigma^B(v_{min})$ is calculated numerically. The lef-tover, non-singular part $\sigma^{SAN}-\sigma^{sing}$ is integrated numerically directly by a Gaussian technique.

3 Numerical results and comparisons

In the second part of this letter we present a series of results from the MC program KORALW and SAN routine KORWAN[1]. We focus on two aspects: study of the

[1]In all of the numerical results presented below we used the following set of input parameters: $1/\alpha_{QED}=137.0359895$, $1/\alpha_W=128.07$, $G_\mu=1.16639\times10^{-5}$ GeV^{-2}, $M_Z=91.1888$ GeV, $\Gamma_Z=2.4974$ GeV, $M_W=80.23$ GeV, $\sin^2\theta_W=\pi\alpha_W/(\sqrt{2}M_W^2G_\mu)=0.23103091$, $\Gamma_W=9G_\mu M_W^3/(6\sqrt{2}\pi)=2.03367033$ GeV. Other parameters are taken from ref. [16]. Also the running width $s\Gamma_Z/M_Z$ is used in the Z propagator, next-to-leading corrections are switched off in the YFS form factor and the final-state masses are set to zero.

technical precision of the KORALW code and the discussion of higher-order ISR corrections. The experimental accuracy of the measurements at LEP2 will be of order 0.5–1%. Therefore it is sufficient to have the theoretical precision of MC code of order 0.1%. Nonetheless in our discussion of the technical precision we will often push the precision even down to 10^{-5}. Is this useful in any sense? Yes, it is! Our comparisons are done almost without cuts. This way the overall results are dominated by paricular parts of phase space. In various 'corners' of phase space there might still be some inaccuracies, contributing below the 0.1% level and harmless in this 'no-cuts' test within the 0.1% precision, but harmful if one starts to impose more stringent cuts enhancing these regions. Pushing the precision to 10^{-5} in our 'no-cuts' tests substantially increases our sensitivity to the 'corners' of the phase space.

Total cross section

The KORALW MC code is quite a complicated program (almost 10,000 lines). Its satisfactory testing poses a highly non-trivial problem. In principle one should cross-check, with at least one completely independent analytical or numerical calculation, *all* the experimentally interesting quantities, of total and differential type, with *all* the possible combinations of cut-offs. This sounds unrealistic (at least for the time being). Therefore we have chosen a somewhat different strategy in testing the KORALW code. To begin with we tried to identify some basic blocks of the program and then perform a series of tests focused on each of these blocks separately. We started with the Born matrix element. Given the fact that, leaving aside ISR corrections, the physics of the Monte Carlo is contained in its matrix element squared, a very powerful cross-check of the physics contents of different generators may be obtained by comparing the values of the matrix element squared evaluated using completely different codes, in phase-space points randomly sampled. The differences due to gauge choices, should manifest themself only in global phases, which are irrelevant if squared matrix element are compared. If the codes assume exactly the same physics ansatz, then the results should agree within the numerical accuracy of the machine used. If this is the case, even using a reduced sample of points, one can be completely sure that the calculations are equivalent. Any difference would reflect either different physics assumptions or just computer-code bugs. We have compared on this *event-by-event* basis the values of Born matrix elements from as many as four different approaches. Namely:

- the KORALW code,
- an alternative computer code which we developed, in which the matrix element squared is built using the techniques described in ref. [17],
- our own computer implementation of the matrix element squared described in ref. [18],
- and finally a custom version of the EXCALIBUR MC program of ref. [4], modified to yield the matrix element squared at a given point of phase-space.

Apart from the purpose of checking the value of the matrix element squared, the use of such a wide variety of calculational approaches served us to dig deeper into the understanding of the structure and properties of the matrix element squared. After some work, we found that, up to an overall constant factor, there was an agreement of 13 digits or better for the total matrix element squared, and for its different spin contributions as well, among the four different approaches. Having checked the Born matrix element we turned to the Born total cross section. This way we were able to check another crucial piece of the algorithm – the Born phase-space integration, i.e. whether the event generation covers the entire phase space, whether the overall and partial normalizations are correct, etc. We compared the MC KORALW results with the SAN results described above and implemented in the KORWAN routine. The results are collected in Table 1. One can see from this table that the typical

Table 1: Born total cross sections: MC (KORALW), SAN (KORWAN) and their ratio

$\sqrt{s}$ GeV	MC KORALW σ_{tot} Born	SAN KORWAN σ_{tot} Born	MC/SAN–1
130	0.079769 ± 0.00001	0.079764 ± 0.00001	0.00007 ± 0.00016
160	3.44770 ± 0.00025	3.44758 ± 0.00001	0.00003 ± 0.00007
176	16.22371 ± 0.00076	16.22463 ± 0.00001	-0.00006 ± 0.00005
190	18.34741 ± 0.00086	18.34912 ± 0.00001	-0.00009 ± 0.00005
205	18.50651 ± 0.00090	18.50783 ± 0.00001	-0.00007 ± 0.00005
300	13.50121 ± 0.00066	13.50157 ± 0.00001	-0.00003 ± 0.00005
500	7.37282 ± 0.00038	7.37308 ± 0.00001	-0.00003 ± 0.00005

agreement $|\sigma^{MC}_{Born}/\sigma^{SAN}_{Born} - 1|$ is better than 10^{-4}, and always within two standard deviations[2].

Having gained some confidence in the Born calculations, we have cross-checked the next piece of the KORALW code – the multiphotonic phase-space integration. As before, we looked at the total cross section but with ISR switched on[3]. The comparison of the second-order exponentiated SAN (with the Δ function of eq. (9)) and the MC total cross sections is given in Table 2. One may notice that for energies close to or below the WW threshold the agreement $|\sigma^{MC}_{ISR}/\sigma^{SAN}_{ISR} - 1|$ is very good – of order 10^{-5}, within the statistical errors. Far above the threshold, however, there appears a systematic deviation between second-order MC and SAN results. How can we explain it? Close to the threshold, only the soft emission is allowed. This soft radiation is properly summed up to all orders both by the MC and SAN formulas. Further above the threshold the situation changes. More hard radiation becomes allowed. Contrary to the soft part, the hard radiation in the SAN formula

[2]The Born level comparison of our semi-analytical program KORWAN with the GENTLE code [19] was reported by D. Bardin at the second plenary LEP2 meeting [20], and agreement between the two programs was at least 7 digits.

[3]Let us mention here that this multiphotonic part of the code is taken without any modifications from the KORALZ code. This greatly reduces the chance of bugs in this piece of the code.

Table 2: $\mathcal{O}(\alpha^2)$ total cross sections: MC (KORALW), Jadach-Ward(JW)-exponentiated SAN (KORWAN) and their ratio

$\sqrt{s}$ GeV	MC KORALW $\sigma_{tot}\ \ \mathcal{O}(\alpha^2)_{exp}$	SAN KORWAN $\sigma_{tot}\ \ \mathcal{O}(\alpha^2)^{JW}_{exp}$	MC/SAN–1
130	0.067009 ± 0.00001	0.067007 ± 0.00001	0.00002 ± 0.00021
160	2.46981 ± 0.00026	2.47002 ± 0.00001	-0.00008 ± 0.00011
176	13.52135 ± 0.00091	13.52211 ± 0.00001	-0.00006 ± 0.00007
190	16.29314 ± 0.00110	16.29277 ± 0.00001	0.00002 ± 0.00007
205	17.08934 ± 0.00118	17.08525 ± 0.00001	0.00024 ± 0.00007
300	13.64190 ± 0.00111	13.64017 ± 0.00001	0.00013 ± 0.00008
500	7.86479 ± 0.00073	7.86084 ± 0.00001	0.00050 ± 0.00009

is truncated exactly on the second order, whereas in the MC formulation some parts of the higher orders are present. These higher-order terms are responsible for the discrepancies in Table 2. To see it more quantitatively, in Table 3 we compare the same second-order MC total cross sections as in Table 2 but with the third-order SAN results (with the Δ function of eq. (13)). It is evident that the discrepancy

Table 3: Total cross sections: $\mathcal{O}(\alpha^2)$ MC (KORALW), Jadach-Ward(JW)-exponentiated $\mathcal{O}(\alpha^3)$ SAN (KORWAN) and their ratio

$\sqrt{s}$ GeV	MC KORALW $\sigma_{tot}\ \ \mathcal{O}(\alpha^2)_{exp}$	SAN KORWAN $\sigma_{tot}\ \ \mathcal{O}(\alpha^3)^{JW}_{exp}$	MC/SAN–1
130	0.067009 ± 0.00001	0.067013 ± 0.00001	-0.00006 ± 0.00021
160	2.46981 ± 0.00026	2.47012 ± 0.00001	-0.00013 ± 0.00011
176	13.52135 ± 0.00091	13.52286 ± 0.00001	-0.00011 ± 0.00007
190	16.29314 ± 0.00110	16.29408 ± 0.00001	-0.00006 ± 0.00007
205	17.08934 ± 0.00118	17.08711 ± 0.00001	0.00013 ± 0.00007
300	13.64190 ± 0.00111	13.64398 ± 0.00001	-0.00015 ± 0.00008
500	7.86479 ± 0.00073	7.86492 ± 0.00001	-0.00002 ± 0.00009

above the threshold disappears. On the other hand such a good agreement as seen in Table 3 should not be taken literally. Instead, it should be considered as an indication that the third-order corrections are of the same order of magnitude and sign as the discrepancy in question. The actual precise cancellation visible in Table 3 may not be true if, for example, one imposes some further cuts or looks at a different observable.

So far we have discussed the MC and SAN results with the focus on technical precision, as the inherent component of the total (physical and technical) error of the MC calculation. The above tables contain however a lot of physical information as well. By inspecting Table 2 versus Table 1, one can see how big the IS photonic corrections to the WW production are. Enquiring further one might ask whether the

second-order corrections, as given in Table 2, are really necessary for the assumed theoretical accuracy of 0.1%? Indeed, the first-order corrections are in this case sufficient, at least for the total cross section, *provided* one uses the multiplicative (JW) exponentiation of ref. [12]. This can be verified by inspecting Table 4, where the same second-order MC results as before are compared with the first-order JW-exponentiated SAN results. The size of the second-order correction is 0.1% in a

Table 4: Total cross sections: $\mathcal{O}(\alpha^2)$ MC (KORALW), Jadach-Ward(JW)-exponentiated $\mathcal{O}(\alpha^1)$ SAN (KORWAN) and their ratio

$\sqrt{s}$ GeV	MC KORALW $\sigma_{tot}\ \ \mathcal{O}(\alpha^2)_{exp}$	SAN KORWAN $\sigma_{tot}\ \ \mathcal{O}(\alpha^1)^{JW}_{exp}$	MC/SAN−1
130	0.067009 ± 0.00001	0.066934 ± 0.00001	0.00111 ± 0.00021
160	2.46981 ± 0.00026	2.46658 ± 0.00081	0.00131 ± 0.00035
176	13.52135 ± 0.00091	13.50562 ± 0.00081	0.00116 ± 0.00009
190	16.29314 ± 0.00110	16.27565 ± 0.00081	0.00107 ± 0.00008
205	17.08934 ± 0.00118	17.06952 ± 0.00081	0.00116 ± 0.00008
300	13.64190 ± 0.00111	13.62754 ± 0.00081	0.00105 ± 0.00010
500	7.86479 ± 0.00073	7.84361 ± 0.00081	0.00270 ± 0.00014

large energy-range. Only for the energies close to 500 GeV does the correction grow to 0.3%. In other exponentiation schemes the second-order ISR might not be negligible. As an example, in Table 5 we show again the second-order MC results but compared with the first-order Kuraev-Fadin (KF) exponentiated SAN results. The discrepancy (i.e. second-order corrections) grows to 0.7% already within the LEP2 energy range.

Table 5: Total cross sections: $\mathcal{O}(\alpha^2)$ MC (KORALW), Kuraev-Fadin(KF)-exponentiated $\mathcal{O}(\alpha^1)$ SAN (KORWAN) and their ratio

$\sqrt{s}$ GeV	MC KORALW $\sigma_{tot}\ \ \mathcal{O}(\alpha^2)_{exp}$	SAN KORWAN $\sigma_{tot}\ \ \mathcal{O}(\alpha^1)^{KF}_{exp}$	MC/SAN−1
130	0.067009 ± 0.00001	0.066695 ± 0.00001	0.00471 ± 0.00021
160	2.46981 ± 0.00026	2.46385 ± 0.00081	0.00242 ± 0.00035
176	13.52135 ± 0.00091	13.46044 ± 0.00081	0.00453 ± 0.00009
190	16.29314 ± 0.00110	16.19217 ± 0.00081	0.00624 ± 0.00008
205	17.08934 ± 0.00118	16.96140 ± 0.00081	0.00754 ± 0.00008
300	13.64190 ± 0.00111	13.51930 ± 0.00081	0.00907 ± 0.00010
500	7.86479 ± 0.00073	7.79601 ± 0.00081	0.00882 ± 0.00014

'Mass loss'

Another interesting observable, which can be calculated within our SAN framework is an average 'mass loss' defined as an average of $v = 1 - s'/s$ variable times $\sqrt{s}/2$, i.e. $(\sqrt{s}/2) \int v d\sigma / \int d\sigma$. In Table 6 we compare, as usual, the second-order

MC and second-order SAN (with the Δ function of eq. (9)) values of the 'mass loss'. One can see from this able that systematic discrepancies between MC and

Table 6: $\mathcal{O}(\alpha^2)$ W-pair 'mass losses', i.e. $<v>\sqrt{s}/2$: MC (KORALW), SAN (KORWAN) and their ratio

$\sqrt{s}$ GeV	MC KORALW $<v>\sqrt{s}/2$ [GeV] $\mathcal{O}(\alpha^2)$	SAN KORWAN $<v>\sqrt{s}/2$ [GeV] $\mathcal{O}(\alpha^2)$	MC/SAN $-$ 1
130	1.37535 ± 0.00148	1.37711 ± 0.00080	-0.00128 ± 0.00122
160	0.53716 ± 0.00029	0.53664 ± 0.00007	0.00097 ± 0.00055
176	1.17741 ± 0.00030	1.17732 ± 0.00008	0.00008 ± 0.00027
190	2.13134 ± 0.00046	2.13053 ± 0.00011	0.00038 ± 0.00022
205	3.18454 ± 0.00066	3.18359 ± 0.00016	0.00030 ± 0.00021
300	10.03224 ± 0.00191	10.02006 ± 0.00048	0.00122 ± 0.00020
500	25.56743 ± 0.00449	25.53362 ± 0.00112	0.00132 ± 0.00018

SAN numbers appear at higher energies. Again, as for the total cross section, these discrepancies can be traced back to the residual third-order terms missing in the SAN result. To see it explicitly we repeat the comparison of Table 6, but with the complete third-order SAN formula (with the Δ function of eq. (13)). Results are given in Table 7. As one may see, the discrepancy changed sign and somewhat

Table 7: W-pair 'mass losses', i.e. $<v>\sqrt{s}/2$: $\mathcal{O}(\alpha^2)$ MC (KORALW), $\mathcal{O}(\alpha^3)$ SAN (KORWAN) and their ratio

$\sqrt{s}$ GeV	MC KORALW $<v>\sqrt{s}/2$ [GeV] $\mathcal{O}(\alpha^2)$	SAN KORWAN $<v>\sqrt{s}/2$ [GeV] $\mathcal{O}(\alpha^3)$	MC/SAN $-$ 1
130	1.37535 ± 0.00148	1.37805 ± 0.00080	-0.00196 ± 0.00122
160	0.53716 ± 0.00029	0.53679 ± 0.00007	0.00070 ± 0.00055
176	1.17741 ± 0.00030	1.17753 ± 0.00008	-0.00010 ± 0.00027
190	2.13134 ± 0.00046	2.13116 ± 0.00011	0.00008 ± 0.00022
205	3.18454 ± 0.00066	3.18499 ± 0.00016	-0.00014 ± 0.00021
300	10.03224 ± 0.00191	10.03286 ± 0.00048	-0.00006 ± 0.00020
500	25.56743 ± 0.00449	25.59021 ± 0.00112	-0.00089 ± 0.00018

decreased in absolute value, showing that the order of magnitude and sign of the effect are consistent with the discrepancy.

Differential distributions

With the help of the SAN formalism outlined earlier we are also able to look at the differential distributions. We start with the photonic distributions $d\sigma/d\log v$ with $v = 1 - s'/s$. In Fig. 1 we show the differential cross section with second-order ISR (with the Δ function of eq. (9)). The histogram shows the MC result. Open circles plot the SAN second-order JW-exponentiated result and the dots plot the difference $(d\sigma^{MC}/d\log v - d\sigma^{SAN}/d\log v) \times 100$ in absolute units. To make it visible

the difference has been multiplied by a factor 100. The errors shown are the MC statistical errors. The plots are for the energies $\sqrt{s} = 190$ GeV and $\sqrt{s} = 500$ GeV. As can be seen, the agreement for 190 GeV is very good, the difference between MC and SAN results being, within statistical errors, consistent with zero. In the case of 500 GeV, one notices a systematic discrepancy in the hard part of the spectrum. This is again the above-mentioned effect of the third-order terms not included in the SAN curve, and present in the MC data. The same pattern can be seen in the next two figures separately for the first- and second-order contributions to the cross section. More precisely, we plot the contributions to $d\sigma/d\log v$ from the second-order $\bar{\beta}_1$ and $\bar{\beta}_2$ terms of the YFS expansion as given in eqs. (11) and (12), respectively. As before, histograms represent the MC results and open circles the SAN results. The difference MC $-$ SAN in absolute units, multiplied by a factor of 100, is plotted with the solid circles. For the $\bar{\beta}_1$ contribution of Fig. 2, again the agreement between SAN and MC is consistent with zero within the statistical errors for the energy 190 GeV, and shows third-order discrepancies for 500 GeV. As for the $\bar{\beta}_2$ contribution of Fig. 3, the discrepancy MC $-$ SAN appears to be larger. It must be noted, however, that the scale in Fig. 3 is changed with respect to Fig. 2. The actual $\bar{\beta}_2$ correction is almost two orders of magnitude smaller than the $\bar{\beta}_1$ one and the absolute size of discrepancies MC $-$ SAN for $\bar{\beta}_2$ and $\bar{\beta}_1$ is the same, reflecting again the third-order differences in MC and SAN calculations.

Finally, we can have a look at the $d\sigma/d\sqrt{s_1}$ distribution, with s_1 being the invariant mass of one of the virtual W bosons. It is rather straightforward to remove one dimension of integration from formula (1) and obtain this single W mass spectrum in the SAN way. A sample comparison of the second-order SAN calculation with our MC program is given in Fig. 4. The SAN result for the difference of $\mathcal{O}(\alpha^2)$ and Born distributions is also given (small dots); note the flip of sign between the two energies shown. The level of discrepancies, consistent with zero, and the size of the initial-state bremsstrahlung effect are clearly visible.

4 Closing remarks

At the end of this letter we would like to add a few words of caution. It may be tempting to interpret the reported high-precision agreement between SAN and MC results as follows: one could conclude that solutions based on the LL Structure Function, either of SAN or MC type, are an excellent approximation of the actual fully exclusive approach, of the YFS/KORALW style. However, this is not necessarily true. First of all, in the LL SF approach one cannot control the transverse momentum distributions, which are not important for the total cross section. Secondly, one has to keep in mind that the Initial-State Radiation constitutes only part of the photonic corrections to the W-pair production. The missing, not factorizable effects of $\mathcal{O}(\alpha)$ cannot be incorporated in the LL SF formalism. On the contrary, these corrections can be taken into account in the exclusive YFS approach in a rather

straightforward way.

Acknowledgements

We thank B.F.L. Ward for stimulating discussions and comments. M.S. thanks E. Fernandez and M. Martinez for their hospitality in IFAE Barcelona, F. Jegerlehner and T. Riemann for their hospitality in DESY-Zeuthen and B. Pietrzyk for his hospitality in LAPP Annecy, within the IN2P3 Collaboration franco-polonaise.

A Appendix

We give here the complete modified formula for σ_0^S of eq. (1), based on ref. [10]:

$$\sigma_0^S(s,s_1,s_2) = C_1G_1 + C_2G_2 + C_3G_3 \tag{18}$$

$$\begin{aligned}
C_1 &= \frac{-2(4\pi\alpha_W)^2}{64\pi s^2 s_1 s_2}\Big[\frac{1}{s^2} + \frac{1}{16}\frac{1}{\sin^4\theta_W}\frac{(1-4\sin^2\theta_W)^2+1}{(s-M_Z^2)^2+s^2\Gamma_Z^2/M_Z^2} \\
&\quad + \frac{1}{2}\frac{1}{\sin^2\theta_W}\frac{1-4\sin^2\theta_W}{s}\frac{s-M_Z^2}{(s-M_Z^2)^2+s^2\Gamma_Z^2/M_Z^2}\Big], \\
C_2 &= \frac{-2(4\pi\alpha_W)^2}{64\pi s^2 s_1 s_2}\frac{1}{8}\frac{1}{\sin^4\theta_W}, \\
C_3 &= \frac{-2(4\pi\alpha_W)^2}{64\pi s^2 s_1 s_2}\Big[-\frac{1}{8}\frac{2-4\sin^2\theta_W}{\sin^4\theta_W}\frac{s-M_Z^2}{(s-M_Z^2)^2+s^2\Gamma_Z^2/M_Z^2} - \frac{1}{2}\frac{1}{\sin^2\theta_W}\frac{1}{s}\Big],
\end{aligned}$$

$$\begin{aligned}
G_1 &= -\lambda^{\frac{3}{2}}\Big[\frac{1}{6}\lambda + 2\Big(s(s_1+s_2)+s_1s_2\Big)\Big], \\
G_2 &= -\lambda^{\frac{1}{2}}\Big[\frac{1}{6}\lambda + 2\Big(s(s_1+s_2)-4s_1s_2\Big)\Big] \\
&\quad +4(s-s_1-s_2)s_1s_2\log\frac{s-s_1-s_2-\lambda^{\frac{1}{2}}}{s-s_1-s_2+\lambda^{\frac{1}{2}}}, \\
G_3 &= -\lambda^{\frac{1}{2}}\Big[\frac{1}{6}\lambda\Big(s+11(s_1+s_2)\Big) + 2\Big(s_1^2+3s_1s_2+s_2^2\Big)s - 2(s_1^3+s_2^3)\Big] \\
&\quad -4\Big(s(s_1+s_2)+s_1s_2\Big)s_1s_2\log\frac{s-s_1-s_2-\lambda^{\frac{1}{2}}}{s-s_1-s_2+\lambda^{\frac{1}{2}}}, \\
\lambda &= (s-s_1-s_2)^2 - 4s_1s_2.
\end{aligned}$$

References

[1] *Z-PHYSICS at LEP 1*, G. Altarelli, R. Kleiss and C. Verzegnassi eds., CERN 89-08, 3 vols.

[2] M. Grünewald, Humboldt Universität Berlin preprint HUB-IEP-95/13.

[3] B. Pietrzyk, in *Tennessee International Symposium on Radiative Corrections: Status and Outlook*, Gatlinburg, Tennessee, USA, June 1994, ed. by B. F. L. Ward (World Scientific, Singapore, 1995) p. 138.

[4] F. A. Berends, R. Pittau, and R. Kleiss, Comput. Phys. Commun. **85**, 437 (1995).

[5] G.Montagna, O. Nicrosini, and F. Piccinini, Comput. Phys. Commun. **90**, 141 (1995).

[6] D. Bardin and T. Riemann, preprint DESY 95-167.

[7] J. Fleischer, K. Kołodziej, and F. Jegerlehner, Phys. Rev. **D47**, 830 (1993).

[8] D. Bardin *et al.*, *Physics at LEP 200*, eds. G. Altarelli, F. Zwirner, (CERN, Geneva, 1995-1996).

[9] M. Skrzypek, S. Jadach, W. Płaczek, and Z. Wąs, Monte Carlo program KORALW 1.02 for W-pair production at LEP2/NLC energies with Yennie-Frautschi-Suura exponentiation, CERN preprint CERN-TH/95-205.

[10] T. Muta, R. Najima, and S. Wakaizumi, Mod. Phys. Lett. **A1**, 203 (1986).

[11] E. A. Kuraev and V. S. Fadin, Sov. J. Nucl. Phys. **41**, 466 (1985).

[12] S. Jadach, M. Skrzypek, and B. F. L. Ward, Phys. Lett. **B257**, 173 (1991).

[13] M. Skrzypek and S. Jadach, Z. Phys. **C49**, 577 (1991).

[14] M. Skrzypek, Acta Phys. Pol. **B23**, 135 (1992).

[15] S. Jadach and B. F. L. Ward, Comput. Phys. Commun. **56**, 351 (1990).

[16] M. Aguilar-Benitez *et al.*, Phys. Rev. **D50**, 1173 (1994).

[17] M. Martinez, R. Miquel, and C. Mana, AIP Conference Proceedings, Particles and Fields Series 39, QED Structure Functions, **no. 201**, 243 (1989).

[18] J. F. Gunion and Z. Kunszt, Phys. Rev. **D33**, 665 (1986).

[19] D. Bardin *et al.*, in *Proceedings of the Zeuthen Workshop on Elementary Particle Theory - Physics at LEP200 and Beyond*, eds. T. Riemann and J. Blümlein (Nucl. Phys. (Proc. Suppl) **B37**, Teuplitz, Germany, 1994).

[20] D. Bardin, The transparencies of the Second General Meeting "WW/eg", CERN June 15-16, 1995,
www page at http://preprints.cern.ch/lep2.2/welcome.html (unpublished).

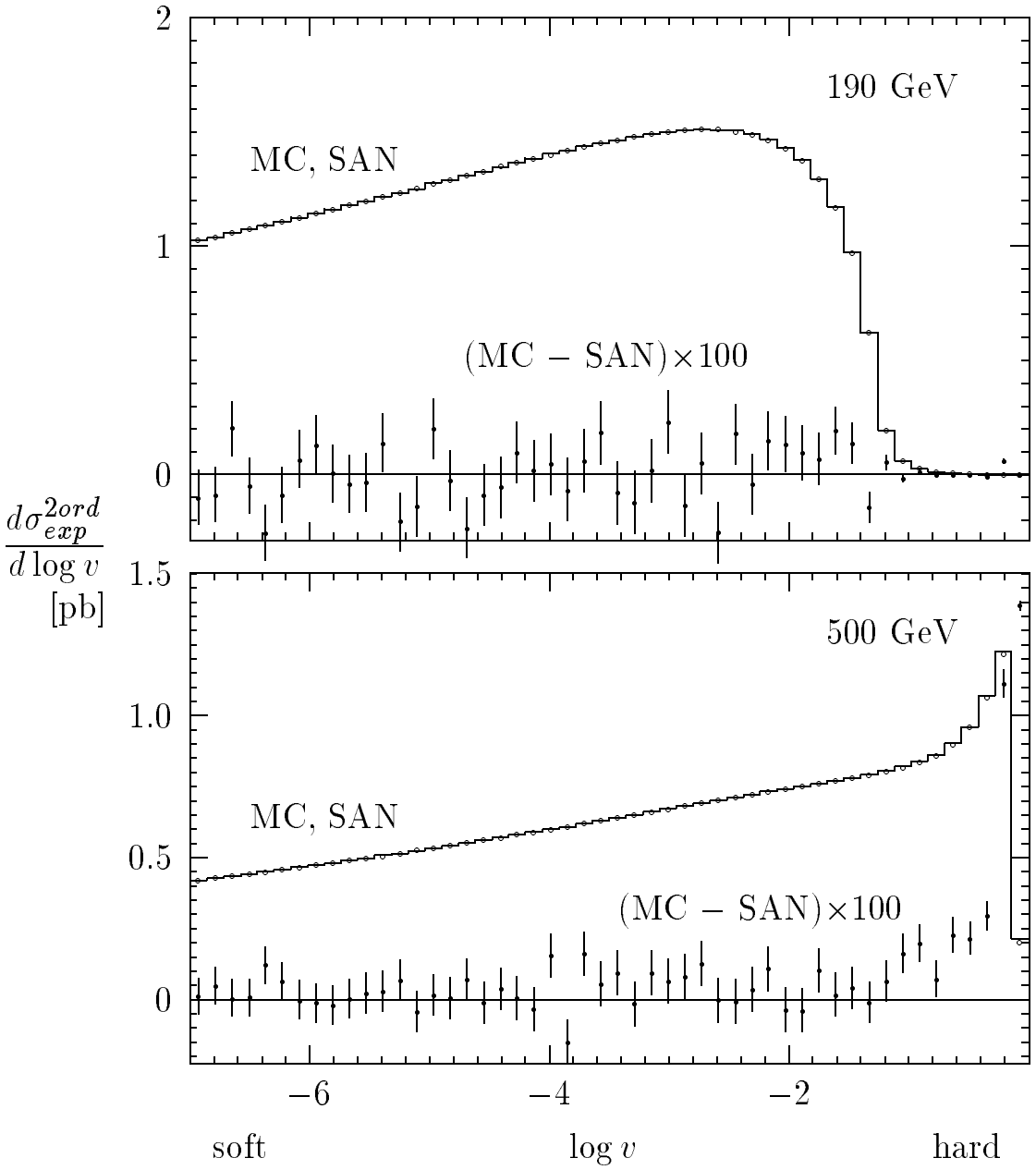

Figure 1: $\mathcal{O}(\alpha^2)$ differential cross sections $d\sigma/d\log v$: MC KORALW (solid line), SAN KORWAN (open circles) and their difference enhanced by a factor 100 (dots). Two energies $\sqrt{s}$ = 190 GeV and 500 GeV are shown.

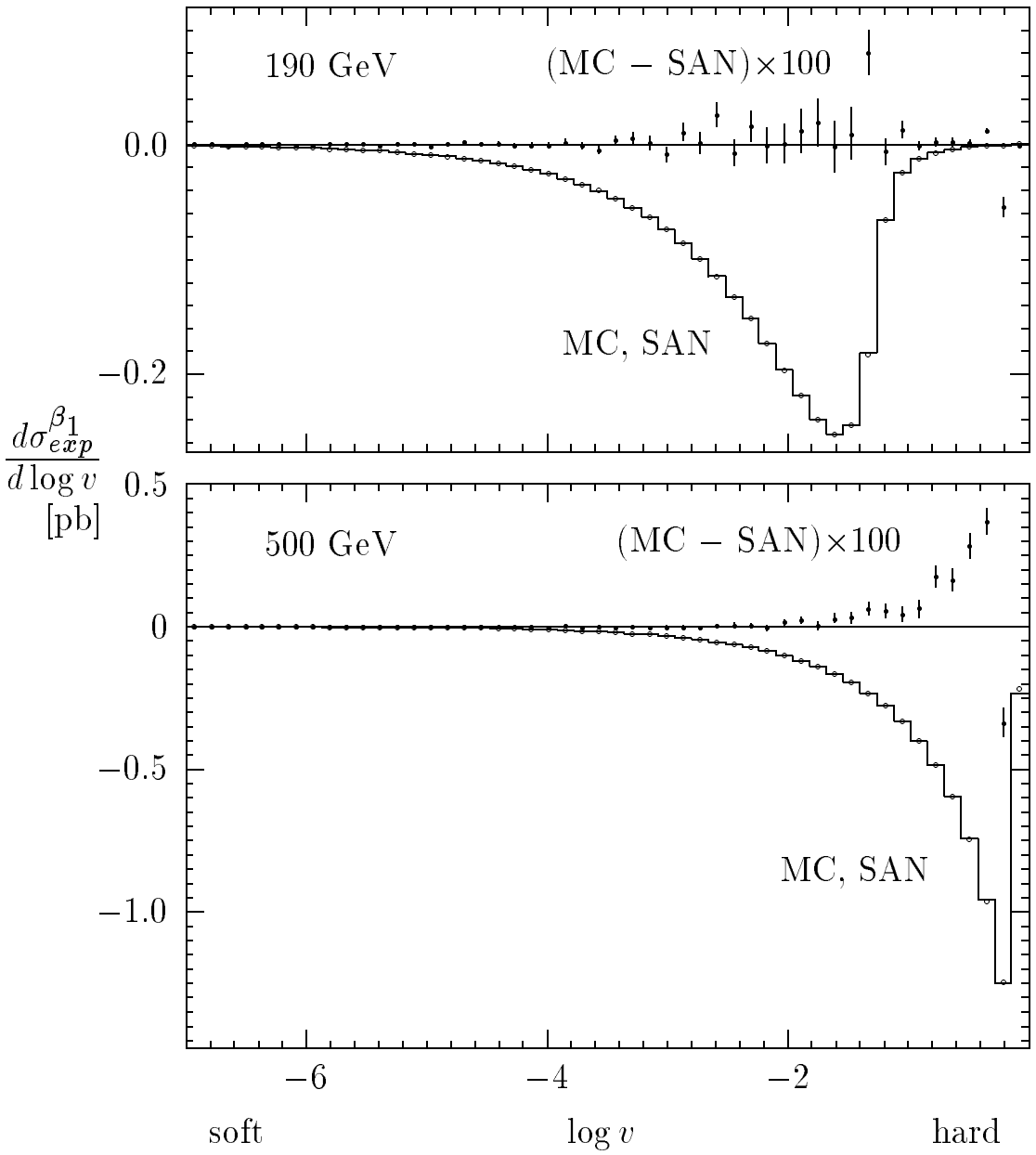

Figure 2: $\mathcal{O}(\alpha^2)$ $\bar{\beta}_1$ contribution to differential cross sections $d\sigma/d\log v$: MC KORALW (solid line), SAN KORWAN (open circles) and their difference enhanced by a factor 100 (dots). Two energies $\sqrt{s}$ = 190 GeV and 500 GeV are shown.

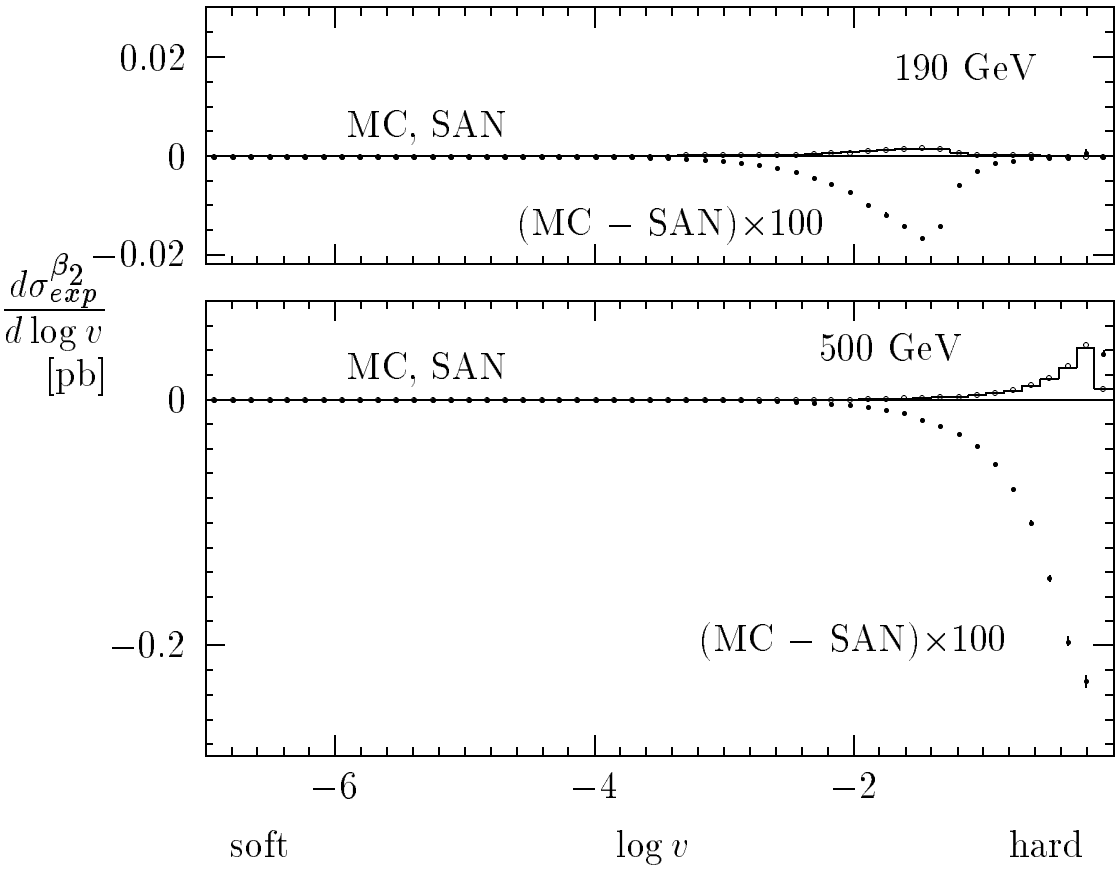

Figure 3: $\mathcal{O}(\alpha^2)$ $\bar{\beta}_2$ contribution to differential cross sections $d\sigma/d\log v$: MC KORALW (solid line), SAN KORWAN (open circles) and their difference enhanced by a factor 100 (dots). Two energies, $\sqrt{s}$ = 190 GeV and 500 GeV, are shown.

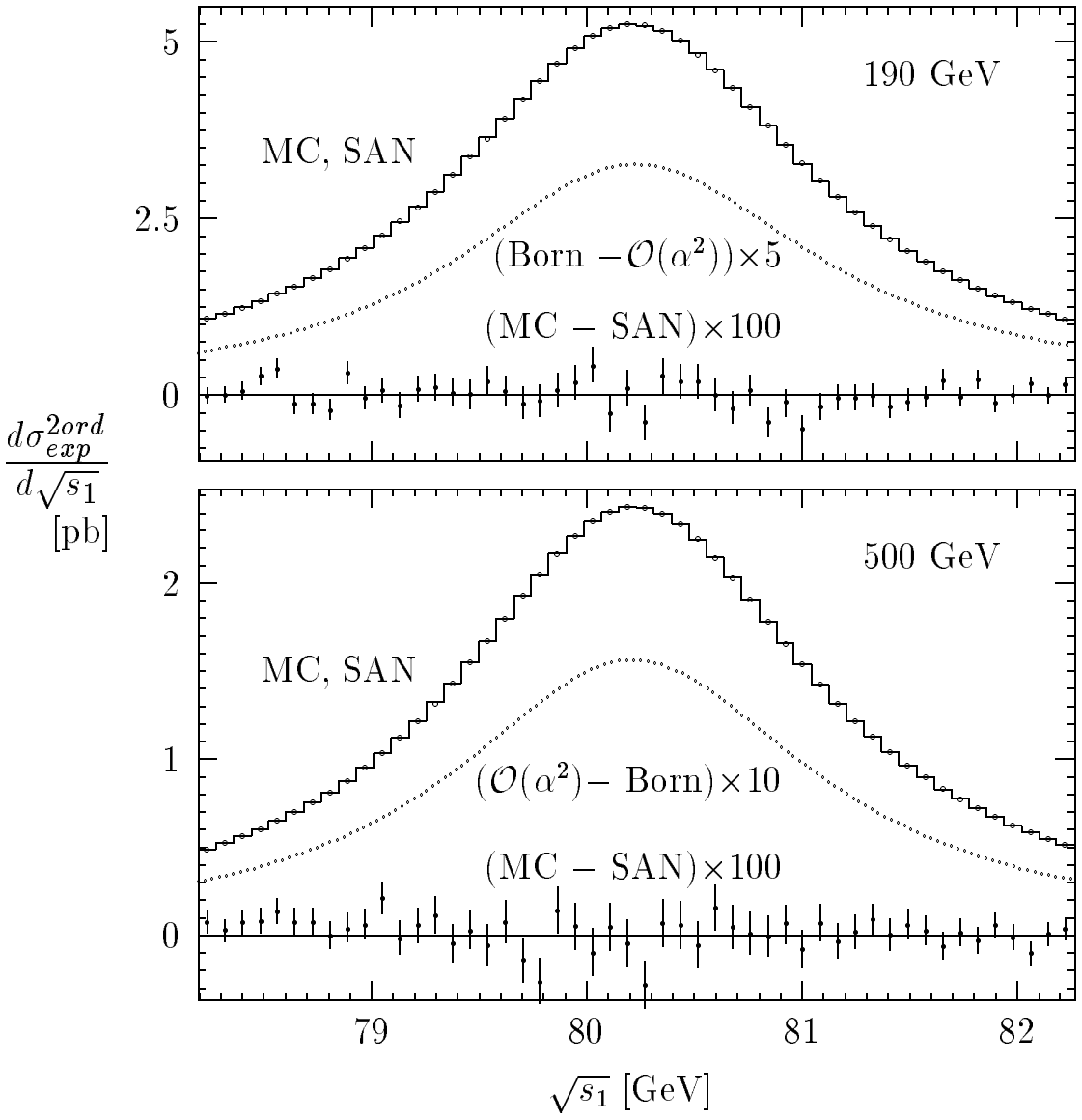

Figure 4: $\mathcal{O}(\alpha^2)$ differential cross sections $d\sigma/d\sqrt{s_1}$: MC KORALW (solid line), SAN KORWAN (open circles), their difference enhanced by a factor 100 (dots) and enhanced SAN difference ($\mathcal{O}(\alpha^2)$−Born) (small dots) are shown for $\sqrt{s}$ = 190 GeV and 500 GeV. Note flip of the sign for SAN ($\mathcal{O}(\alpha^2)$−Born) difference and the two $\sqrt{s}$.